Metabolic Control of Recombinant Protein *N*-Glycan Processing in NS0 and CHO Cells

Kym N. Baker,[1,2] Mark H. Rendall,[1,2] Anna E. Hills,[1] Michael Hoare,[2] Robert B. Freedman,[1] David C. James[1]

[1]Department of Biosciences, University of Kent, Canterbury, Kent CT2 7NJ, UK; telephone: +44-1227-823746; fax: +44-1227-763912; e-mail: d.c.james@ukc.ac.uk
[2]The Advanced Centre for Biochemical Engineering, Department of Chemical and Biochemical Engineering, University College London, London, UK

Received 15 May 2000; accepted 28 September 2000

Abstract: Chinese hamster ovary and murine myeloma NS0 cells are currently favored host cell types for the production of therapeutic recombinant proteins. In this study, we compared *N*-glycan processing in GS-NS0 and GS-CHO cells producing the same model recombinant glycoprotein, tissue inhibitor of metalloproteinases 1. By manipulation of intracellular nucleotide-sugar content, we examined the feasibility of implementing metabolic control strategies aimed at reducing the occurrence of murine-specific glycan motifs on NS0-derived recombinant proteins, such as Galα1,3Galβ1,4GlcNAc. Although both CHO and NS0-derived oligosaccharides were predominantly of the standard complex type with variable sialylation, 30% of *N*-glycan antennae associated with NS0-derived TIMP-1 terminated in α1,3-linked galactose residues. Furthermore, NS0 cells conferred a greater proportion of terminal *N*-glycolylneuraminic (sialic) acid residues as compared with the *N*-acetylneuraminic acid variant. Inclusion of the nucleotide-sugar precursors, glucosamine (10 m*M*, plus 2 m*M* uridine) and *N*-acetylmannosamine (20 m*M*), in culture media were shown to significantly increase the intracellular pools of UDP-*N*-acetylhexosamine and CMP-sialic acid, respectively, in both NS0 and CHO cells. The elevated UDP-*N*-acetylhexosamine content induced by the glucosamine/uridine treatment was associated with an increase in the antennarity of *N*-glycans associated with TIMP-1 produced in CHO cells but not *N*-glycans associated with TIMP-1 from NS0 cells. In addition, elevated UDP-*N*-acetylhexosamine content was associated with a slight decrease in sialylation in both cell lines. The elevated CMP-sialic acid content induced by *N*-acetylmannosamine had no effect on the overall level of sialylation of TIMP-1 produced by both CHO and NS0 cells, although the ratio of *N*-glycolylneuraminic acid:*N*-acetylneuraminic acid associated with NS0-derived TIMP-1 changed from 1:1 to 1:2. These data suggest that manipulation of nucleotide-sugar metabolism can promote changes in *N*-glycan processing that are either conserved between NS0 and CHO cells or specific to either NS0 cells or CHO cells. © 2001 John Wiley & Sons, Inc. *Biotechnol Bioeng* **73**: 188–202, 2001

Keywords: glycosylation; high-performance liquid chromatography (HPLC); Chinese hamster ovary (CHO) cells; murine myeloma cells; sialic acid; α-galactose; nucleotide sugar

Correspondence to: D. James

INTRODUCTION

A number of reports have demonstrated mammalian host-cell-specific processing of *N*-glycans associated with recombinant proteins (James et al., 1995; Lifely et al., 1995). These differences may be important for therapeutic proteins as they can directly alter the antigenicity, rate of clearance in vivo, and stability of recombinant proteins (Jenkins et al., 1996). Thus, it is important not only to be able to characterize glycans bound to a therapeutic recombinant protein to predict the consequences for in vivo efficacy, but also to understand the cellular controls underpinning glycan processing in a potential host cell enabling the implementation of appropriate strategies to control cellular glycosylation (Grabenhorst et al., 1999; James and Baker, 1999).

To date, only a very limited number of studies have described the glycosylation of recombinant proteins produced by murine cell types. In contrast to human, Chinese hamster ovary (CHO), and baby hamster kidney (BHK) cells, *N*-glycans produced in murine (e.g., hybridomas, NS0, and C127) cell types may be associated with α-linked galactose residues (Galα1,3Galβ1,4GlcNAc; Sheeley et al., 1997), which are absent in old world monkeys, apes, and humans, and are consequently immunogenic (Lavecchio et al., 1995). In addition, murine cell lines have a tendency to confer *N*-glycolylneuraminic acid (NeuGc), an oncofetal antigen and potentially immunogenic derivative of *N*-acetylneuraminic acid (NeuAc). NeuGc has been found to be associated with the oligosaccharides of an immunoglobulin M (IgM) produced by a human–mouse hybridoma, where it was twice as prevalent as NeuAc (Monica et al., 1995). Similarly, comparison of glycans associated with a chimeric immunoglobulin G (IgG) produced by CHO and NS0 cells revealed modification of NS0-derived glycans with NeuGc, but not NeuAc. This was linked to enhanced

© 2001 John Wiley & Sons, Inc.

FORMYCON-1084

rate of plasma clearance (Marzowski et al., 1995). In these cases, the proteins investigated were generally antibodies, where *N*-glycan processing is sterically hindered at Asn_{297} in the Fc region (Jefferis and Lund, 1997). Antibodies are therefore not an ideal model to investigate the complete potential of NS0 cells for *N*-glycan processing.

In this study, we examine the ability of murine myeloma NS0 cells to process the *N*-glycans of a model recombinant protein, human tissue inhibitor of metalloproteinases 1 (TIMP-1). Both *N*-glycosylation sites of recombinant TIMP-1 (Asn_{30} and Asn_{78}) produced by CHO cells are known to exhibit extensive microheterogeneity (Sutton et al., 1994), and structural analysis has confirmed no steric hindrance to glycosylation (GomisRuth et al., 1997). This protein is therefore an ideal model for direct comparison of *N*-glycan processing in murine NS0 cells with *N*-glycan processing in the well-characterized CHO cell (i.e., we can analyze the complete repertoire of *N*-glycans that NS0 cells will confer). To this end, we have utilized both NS0 and CHO cell lines producing recombinant human TIMP-1 at specific productivities in excess of 20 $\mu g\ 10^6\ cells^{-1}\ day^{-1}$, which is more relevant to industrial processes. In both cases, TIMP-1 expression is under glutamine synthetase selection/amplification (Cockett et al., 1990). Consequently, ammonia does not accumulate in these cultures so we can effectively eliminate the well-documented effect of this toxic metabolite on *N*-glycan processing (Gawlitzek et al., 1998; Valley et al., 1999; Zanghi et al., 1998). By manipulation of intracellular nucleotide-sugar content, which is known to be involved in the regulation of *N*-glycan processing, we examined the feasibility of implementing metabolic control strategies aimed at reducing the occurrence of murine-specific glycan motifs on NS0-derived recombinant proteins. This report identifies conserved features and differences in metabolic control of *N*-glycan processing in CHO and NS0 cell lines.

MATERIALS AND METHODS

Cell Lines, Culture Conditions, and Recombinant Protein Production

NS0 and CHO cell lines expressing recombinant TIMP-1 under glutamine synthetase selection and amplification were kindly donated by Celltech Therapeutics, plc (Slough, UK). Both cell lines were created as described extensively by Cockett et al. (1990). The GS-CHO cell line used was a suspension-adapted variant, 19.6(500)14. Both TIMP-1–secreting cell lines were routinely maintained at 37°C in a 5% CO_2 atmosphere in 1-L spinner flasks (Techne, Cambridge, UK) with a working culture volume of 0.4 L in glutamine-free Dulbecco's modified essential medium/nutrient mix F12 (DMEM-F12) supplemented with 2% (v/v) fetal calf serum (FCS; Gibco BRL); 25 μM methionine sulfoxamine; 60 $\mu g\ mL^{-1}$ L-glutamic acid; 60 $\mu g\ mL^{-1}$ L-asparagine; and 7 $\mu g\ mL^{-1}$ each of adenosine, guanosine, cytidine, and uridine; and 2.4 $\mu g\ mL^{-1}$ thymidine (Sigma Chemical Co., Poole, UK). Viable cell density was assessed daily using the trypan blue exclusion method. For metabolic manipulation experiments, the medium defined earlier for GS-CHO and GS-NS0 cell growth was supplemented with either *N*-acetylmannosamine (Sigma; 20 m*M*) or glucosamine (Sigma; 10 m*M*) plus uridine (Sigma; 2 m*M*) at the beginning of the exponential growth phase of culture (24 h). Glucose consumption, lactate production, and ammonia accumulation were measured using standard enzyme-linked colorimetric assay kits (glucose, hexokinase; lactate, lactate dehydrogenase; ammonium, glutamate dehydrogenase; all purchased from Sigma) according to manufacturer's instructions.

Quantitation and Immunoaffinity Purification of Recombinant TIMP-1

Recombinant TIMP-1 was quantified using a BIAcore 2000 optical biosensor (BIOcore, Herts., UK) (Baker et al., 1997). Following centrifugation of either GS-NS0 or GS-CHO cell broth at 1000*g* for 10 min at 4°C, recombinant TIMP-1 was purified by immunoaffinity chromatography using anti–TIMP-1 monoclonal antibody MAC019 (kindly donated by Celltech) covalently conjugated to CNBr-activated Sepharose 4B (Sigma). Cell-free supernatant was passed over a 1.5-mL bed volume column and contaminating proteins were removed by washing with 5 column volumes of phosphate-buffered saline (pH 7.0) at 1 mL min^{-1}. Recombinant TIMP-1 was eluted with 5 column volumes of 0.1 *M* glycine-HCl (pH 3.0), and immediately neutralized to pH 7.0 by the addition of 1 *M* Tris-HCl (pH 9.0). Purified TIMP-1 was desalted into water using a PD-10 desalting column (Amersham Pharmacia), lyophilized, and stored at −20°C. TIMP-1 was routinely found to be >95% pure after analysis by sodium dodecylsulfate– polymerase gel electrophoresis (SDS-PAGE).

N-Glycan Release, Recovery, and Derivatization with 2-Aminobenzamide

Recombinant TIMP-1 (500 μg) protein was digested with PNGase F in a 96-well-plate PVDF format following standard procedures (Papac et al., 1998), except that acetic acid incubation was not undertaken. Released *N*-glycans were removed from the deglycosylated TIMP-1 polypeptide (which remain bound to the 96-well plate) by aspiration, then concentrated and desalted by lyophilization. *N*-glycans released from TIMP-1 protein were reductively aminated at the reducing terminus with the fluorophore 2-aminobenzamide (2-AB; excitation 330 nm, emission 420 nm) using a kit supplied by Oxford GlycoSciences, Ltd. (Abingdon, UK). All procedures were carried out according to manufacturer's instructions.

Matrix-Assisted Laser Desorption Mass Spectrometry of 2-AB Derivatized *N*-Glycans

After labeling with 2-aminobenzamide, enzymatically desialylated neutral *N*-glycans were analyzed as sodiated mo-

10970290, 2001, 3, Downloaded from https://analyticalsciencejournals.onlinelibrary.wiley.com/doi/10.1002/bit.1051 by University Of Manitoba, Wiley Online Library on [25/10/2024]. See the Terms and Conditions (https://onlinelibrary.wiley.com/terms-and-conditions) on Wiley Online Library for rules of use; OA articles are governed by the applicable Creative Commons License

RIGHTSLINK

lecular ions ([M + Na]$^+$) in positive ion mode using 2,3-dihydroxybenzoic acid (Aldrich) as matrix as described previously (James and Jenkins, 1997).

Enzymatic Digestion of Released *N*-Glycans

To desialylate *N*-glycans, 1 μL (containing approximately 1 nmol) of an *N*-glycan mixture was incubated with 0.02 U sialidase from *Arthrobacter ureafaciens* (Oxford GlycoSciences) in 2 m*M* sodium acetate buffer (pH 5.0), overnight at room temperature. Following desialylation, removal of terminal α-linked galactose residues with green coffee bean α-galactosidase (Oxford GlycoSciences) was performed following the manufacturer's instructions. Reactions were terminated by freezing in liquid nitrogen prior to analysis by MALDI-MS as described previously.

Analysis of *N*-Glycans by Normal Phase HPLC

Separation of released *N*-glycans according to their hydrodynamic volume was performed using an Tosohaas TSK Amide-80 column (4.6 × 250 mm; Anachem, UK) according to the method of Guile et al. (1996). Initial conditions were 35% solvent A (50 m*M* ammonium formate, pH 4.4), 65% solvent B (100% CH_3CN) at 0.4 mL min^{-1} for 5 min, followed by a linear gradient of 35% to 53% solvent A over 72 min, then 53% to 100% solvent A over the next 3 min. The flow rate was then increased to 1 mL min^{-1} over 2 min and the column washed in 100% solvent A for 5 min followed by re-equilibration in 35% solvent A. Oligosaccharide elution was monitored with a Waters 474 scanning fluorescent detector. Separations were calibrated using a standard 2-AB-labeled dextran ladder (Oxford GlycoSciences) and resolved glycans were assigned glucose unit values accordingly.

Analysis of Sialylated *N*-Glycans by Cation-Exchange HPLC

2-AB-labeled *N*-glycans were separated into neutral, mono-, di-, tri-, or tetrasialylated structures by HPLC with a Glycosep C cation-exchange column (4.6 × 100 mm; Oxford GlycoSciences). Using this procedure, neutral oligosaccharides elute in the void volume, whereas charged *N*-glycans are progressively eluted using a linear gradient of 100% solvent A (20% CH_3CN, 80% H_2O) to 100% solvent B (20% CH_3CN, 80% 250 m*M* ammonium formate, at pH 4.5) at a flow rate of 0.3 mL min^{-1} over 35 min. Oligosaccharide elution was monitored with a Waters 474 scanning fluorescence detector. Separations were calibrated using standard 2-AB-labeled oligosaccharides from Oxford GlycoSciences.

Analysis of Sialic Acid Variants by Reverse-Phase HPLC

Quantitative analysis of the extent to which recombinant TIMP-1 proteins were substituted with either *N*-glycolylneuraminic (NeuGc) and *N*-acetylneuraminic (NeuAc) sialic acid variants was achieved by release (using mild acid hydrolysis) and labeling of sialic acids with the fluorophore 1,2-diamino-4,5-methylenedioxybenzene (DMB) using a kit supplied by Oxford GlycoSciences, according to the manufacturer's instructions. The DMB-derivatized sialic variants were then separated by rpHPLC on a Waters 626 system using a Phenomenex Jupiter C_{18} column (250 × 2 mm, particle size 5 μm) with a linear gradient of 5% CH_3CN, 7% MeOH to 10% CH_3CN, 7% MeOH over 40 min at 0.4 mL min^{-1}. Variants were identified by comparision of their retention time with that of DMB-labeled standards.

Sialyltransferase Assay

This assay was carried out as previously described (Hooker et al., 1999) with the following exceptions; 1 × 10^8 cells from either NS0 or CHO cultures were used for each experiment and a sialidase inhibitor (1 m*M* 2,3-dehydro-2-deoxy-*N*-acetylneuraminic acid) was included in the reaction mix. Briefly, total sialyltransferase activity of the solubilized cellular lysate was assayed for its ability to catalyze the addition of CMP-fluoresceinyl-NeuAc onto asialofetuin. The reaction was halted by the addition of 0.1 *M* CTP, a potent inhibitor of sialyltransferase. The incorporation of CMP-9-fluoresceinyl-NeuNAc into the acceptor glycoprotein was monitored by separation of bound from free fluoresceinyl-NeuNAc (excitation 490 nm, emission 520 nm) on a "Fast Desalt" gel-filtration column (Amersham Pharmacia) attached to a Waters 626 HPLC system. The degree of incorporation of CMP-9-fluoresceinyl-NeuNAc into asialofetuin was determined by comparison to a standard curve generated with purified α2,3-sialyltransferase protein of known specific activity (Sigma). One unit of activity is defined as that which will transfer 1 μmol of NeuAc from CMP-NeuAc to an acceptor per minute at 37°C at pH 6.5.

Extraction and Separation of Soluble Nucleotide Sugars

Soluble nucleotides were extracted from the cells and separated by anion-exchange HPLC using a modified protocol, similar to that described by Pels Rijcken et al. (1995). Cells (1 × 10^8) were harvested by centrifugation (3000*g* for 10 min at 4°C) and washed twice with PBS. The cells were then incubated with 15 mL of cold ethanol (75% [v/v], 4°C) for 15 min, followed by centrifugation (12,000*g* for 25 min at 4°C). The pellet was washed twice with 3 mL of cold ethanol (75% [v/v] 4°C), vortexed briefly, and the extract and washes recentrifuged under vacuum to dryness for 2 h at 4°C. Chloroform:methanol:water (10:5:3; 4.5 mL) was added to extract the lipids and vortexed briefly. Following centrifugation (3000*g* for 10 min at 4°C), the upper phase (~1.5 mL) was carefully removed and the lower phase was washed with 1.5 mL methanol/water (1:1 [v/v]) and recentrifuged. The upper phase and wash were then centrifuged

10970290, 2001, 3, Downloaded from https://analyticalsciencejournals.onlinelibrary.wiley.com/doi/10.1002/bit.1051 by University Of Manitoba, Wiley Online Library on [25/10/2024]. See the Terms and Conditions (https://onlinelibrary.wiley.com/terms-and-conditions) on Wiley Online Library for rules of use; OA articles are governed by the applicable Creative Commons License

RIGHTSLINK

under vacuum to dryness for 2 h at 4°C. Anion-exchange chromatography of soluble nucleotides was performed using a Whatman Partisphere SAX cartridge (4.6 mm × 125 mm, particle size 5 μm) linked to a Waters 626 HPLC system (Millipore, Ltd., Watford, UK), which was controlled using MILLENIUM software. Separations employed a three-step linear gradient using phosphate buffer solvents from 5 m*M* H_3PO_4/KH_2PO_4 (pH 4.0) (solvent A) to 0.5 *M* KH_2PO_4/K_2HPO_4 (pH 4.5) (solvent B); 0% to 10% B over 30 min, 10% to 45% B over 15 min, and 45% to 100% B over 10 min at 1.0 mL min^{-1}. Peaks detected at 262 nm were identified and calibrated against nucleotide-sugar standards of known concentration.

RESULTS

Culture of GS-NS0 and GS-CHO Cells

For the purpose of the comparative experiments described in this study, GS-NS0 or GS-CHO cells were cultured in 1-L spinner vessels with a 400-mL culture volume. Cultures were seeded at 2×10^5 cells mL^{-1} from cell cultures in mid-exponential phase growth. Additions (*N*-acetylmannosamine [ManNAc] or glucosamine *plus* uridine [GlcN + Urd]) to the culture were made after 24-h growth and product harvested after a further 48-h growth, corresponding to middle to late phase exponential growth. Typical data for cell growth in the different environmental conditions employed are shown in Figure 1. For all cultures, cell viability was routinely >90% (data not shown).

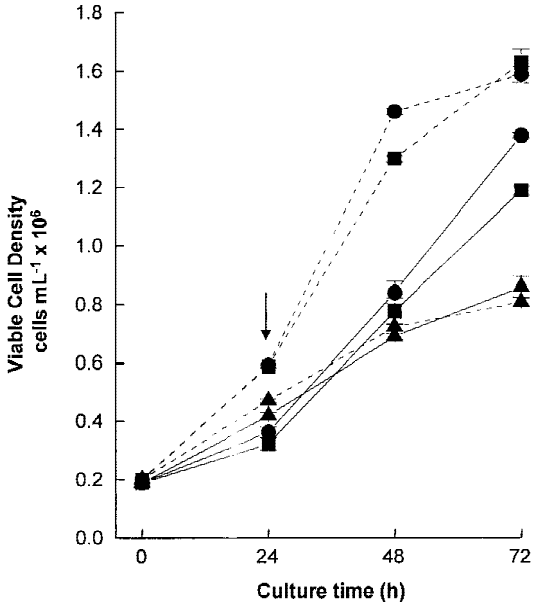

Figure 1. Growth of GS-NS0 and GS-CHO cells in culture. GS-NS0 (broken lines) and GS-CHO (unbroken lines) cells were seeded at 2×10^5 cells mL^{-1} and grown without further additions to the culture (control, ■) or supplemented after 24-h growth (arrow) with 20 m*M* *N*-acetylmannosamine (ManNAc, ●) or 10 m*M* glucosamine plus 2 m*M* uridine (GlcN + Urd, ▲). Data are the mean of duplicate cultures ± SE.

Clear differences in cell growth characteristics were evident. The GS-NS0 cells attained a higher viable cell density earlier in culture than the GS-CHO cells, which exhibited a characteristic lag phase. For both cell types, maximal rates of cell growth occurred between 24 and 48 h of culture (control: mean GS-NS0, $\mu = 0.033\ h^{-1}$, $t_d = 20.9$ h; mean GS-CHO, $\mu = 0.037\ h^{-1}$, $t_d = 18.8$ h), after which NS0 cell growth slowed relative to CHO cell growth. Addition of 20 m*M* *N*-acetylmannosamine to either GS-NS0 or GS-CHO cultures after 24 h had no subsequent effect on cell growth, whereas addition of 10 m*M* glucosamine *plus* 2 m*M* uridine had an obvious inhibitory effect (GlcN + Urd: mean GS-NS0, $\mu = 0.028\ h^{-1}$, $t_d = 24.8$ h; mean GS-CHO, $\mu = 0.021\ h^{-1}$, $t_d = 33.1$ h). These cell growth data were accompanied by reductions in cell-specific glucose consumption after administration of GlcN + Urd. Between 24 and 72 h of culture, mean $q_{glucose}$ in NS0 and CHO cultures (plus or minus ManNAc) varied between 0.145 and 0.195 μmol 10^6 $cells^{-1}$ day^{-1}, whereas mean $q_{glucose}$ in the GlcN + Urd cultures ranged from 0.06 (GS-NS0) to 0.09 μmol 10^6 $cells^{-1}$ day^{-1} (GS-CHO) over the same period. Ammonia accumulation in both GS cell lines was consistently below 0.15 m*M* (data not shown).

Recombinant TIMP-1 secretion was assessed by direct measurement of the rate of binding of recombinant protein to immobilized monoclonal anti–TIMP-1 using an optical biosensor (data not shown). At 72-h growth of control or ManNAc-treated GS-NS0 and GS-CHO cultures, recombinant protein had accumulated to a similar level (GS-NS0, ~20 μg mL^{-1}; GS-CHO, ~30 μg mL^{-1}). Maximum cell-specific productivity during this period of cell growth was slightly greater for GS-CHO cells ($q_{TIMP\text{-}1} = 25.9$ μg 10^6 $cells^{-1}$ day^{-1}) than for the GS-NS0 cells ($q_{TIMP\text{-}1} = 21.2$ μg 10^6 $cells^{-1}$ day^{-1}). Addition of GlcN + Urd compromised recombinant protein yield significantly; that is, there was a 45% reduction from GS-CHO cultures and a 29% reduction from GS-NS0 cultures.

Comparative Analysis of *N*-Glycans Associated with Recombinant TIMP-1 Produced by GS-NS0 and GS-CHO Cells

For both NS0- and CHO-cell-derived recombinant TIMP-1 glycoproteins recovered after 72-h culture, we quantitatively analyzed the key sources of *N*-glycan microheterogeneity, specifically the degree of antennarity (or branching), α1–3-linked galactosylation and terminal sialylation. These analyses are summarized in Figures 2 to 5 and Tables I to V. Prior to most analyses of *N*-glycans released from immunoaffinity-purified TIMP-1, we labeled the reducing terminus with the fluorophore 2-aminobenzamide (Bigge et al., 1995). This permitted sensitive quantitative analyses of the both neutral core (Fig. 2) and acidic sialylated (Fig. 4) *N*-glycan populations by HPLC.

As shown in Figure 2, preliminary analyses of the desialylated *N*-glycans by normal phase HPLC showed that NS0-derived *N*-glycans were more heterogeneous. Struc-

10970290, 2001, 3, Downloaded from https://analyticalsciencejournals.onlinelibrary.wiley.com/doi/10.1002/bit.1051 by University Of Manitoba, Wiley Online Library on [25/10/2024]. See the Terms and Conditions (https://onlinelibrary.wiley.com/terms-and-conditions) on Wiley Online Library for rules of use; OA articles are governed by the applicable Creative Commons License

RIGHTSLINK

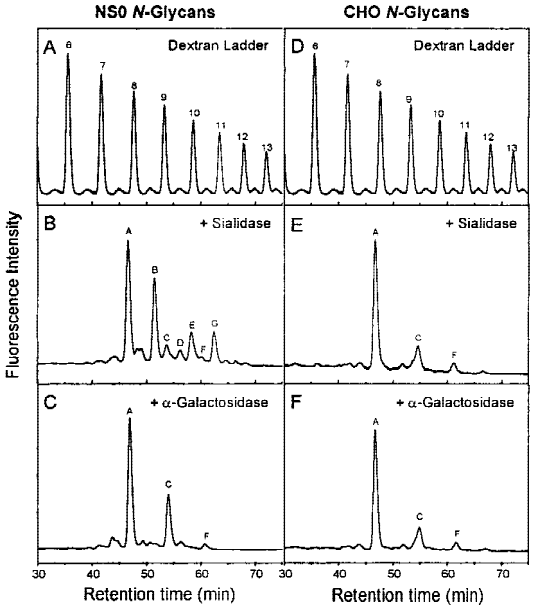

Component	Glucose unit value	Predicted *N*-glycan structure
A	7.7	A2G2F
B	8.5	A2G3F
C	9.0	A3G3F
D	9.5	A2G4F
E	9.9	A3G4F
F	10.4	A4G4F
G	10.8	A3G5F

Figure 2. Separation of fluorophore-labeled *N*-glycans released from recombinant TIMP-1 produced in GS-NS0 and GS-CHO cells by normal phase HPLC. *N*-glycans were released from recombinant TIMP-1 proteins by peptide-*N*-glycosidase F and labeled at the reducing terminus with 2-aminobenzamide. Panels (A) and (D) show representative separations of 2-aminobenzamide-derivatized dextran ladder standards used to calculate the hydrodynamic volume (expressed as a glucose unit value indicated above each peak) of resolved *N*-glycans. Each component (*N*-glycan) of a chromatogram was assigned a structure based on the calculated glucose unit value as described extensively by Guile et al. (1996). Desialylated *N*-glycan populations are shown in (B) and (E); α1,3-linked galactose residues were confirmed by digestion of the *N*-glycan population with sialidase *plus* α-galactosidase (C, F). A, number of antennae; G, number of galactose residues; F, number of deoxyhexose (fucose) residues; S, number of sialic acid residues.

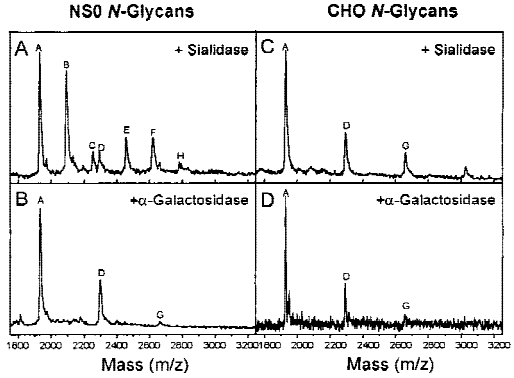

Component	Observed molecular mass (Da)	Correlating molecular mass (Da)	Predicted *N*-glycan structure
A	1931	1930.6	A2G2F
B	2091	2092.7	A2G3F
C	2254	2254.9	A2G4F
D	2296	2295.9	A3G3F
E	2459	2458.0	A3G4F
F	2619	2620.1	A3G5F
G	2661	2661.3	A4G4F
H	2783	2782.4	A3G6F

Figure 3. Analysis of fluorophore-labeled *N*-glycans released from recombinant TIMP-1 produced in GS-NS0 and GS-CHO cells by MALDI-MS. *N*-linked oligosaccharides were released by digestion with peptide-*N*-glycosidase F, derivatized with 2-aminobenzamide at the reducing terminus (+120 Da), and approximately 0.5 pmol of the mixture analyzed as $[M + Na]^+$ ions (+23 Da) by MALDI-TOF MS in positive ion mode. A predicted *N*-glycan structure (nomenclature as described in Fig. 2) for each component with a given observed molecular mass was derived from the correlating molecular mass of an *N*-glycan with defined monosaccharide composition using basic biosynthetic principles.

tural assignments were made on the basis of hydrodynamic volume (determined as glucose units) after comparison with the retention time of dextran standards. This method has been described extensively (Guile et al., 1996; Rudd et al., 1997). Limited exoglycosidase digestion with sialidase alone, or in combination with α-galactosidase, revealed the distribution of core oligosaccharides to be similar, consisting of predominantly fucosylated bigalactosylated biantennary structures (A2G2F) with smaller proportions of triantennary (A3G3F) and tetraantennary variants (A4G4F). These assignments were confirmed by comparable MALDI-MS analyses of the 2-aminobenzamide-labeled oligosaccharides (Fig. 3). The relative proportions of *N*-glycans with varying antennarity is shown in Table I. Clearly, in control conditions (no addition of nucleotide-sugar precursors), TIMP-1 produced by GS-CHO cells was associated with a greater proportion of tetraantennary oligosaccharides (11% of the *N*-glycan pool) than the protein produced by GS-NS0 cells (3% of the *N*-glycan pool). However, these different proportions did not greatly affect the calculated mean number of antennae per *N*-glycan given in Table III (approximately 2.4 to 2.5 antennae per *N*-glycan).

Digestion of the desialylated *N*-glycan pool by green coffee bean α-galactosidase unambiguously demonstrated that α1,3-linked galactose residues were exclusively associated only with NS0-derived *N*-glycans. Taking into account the structural assignments made possible by normal phase HPLC (Fig. 2) and confirmed by MALDI-MS analysis of monosaccharide composition (Fig. 3), α1,3-linked galactose residues were associated with specific bi- and triantennary components (components B [A2G3F], D [A2G4F], E [A3G4F], and G [A3G5F] in Fig. 2). As for quantitation of antennarity, integration of the normal phase peak areas permitted calculation of molar α-Gal content, expressed as mol

10970290, 2001, 3, Downloaded from https://analyticalsciencejournals.onlinelibrary.wiley.com/doi/10.1002/bit.1051 by University Of Manitoba, Wiley Online Library on [25/10/2024]. See the Terms and Conditions (https://onlinelibrary.wiley.com/terms-and-conditions) on Wiley Online Library for rules of use; OA articles are governed by the applicable Creative Commons License

RIGHTSLINK

Table I. Effect of nucleotide-sugar precursor addition to cultures of GS-NS0 and GS-CHO cells on the antennarity of *N*-glycans associated with recombinant TIMP-1.

Treatment group		Biantennary *N*-glycans (%)	Triantennary *N*-glycans (%)	Tetraantennary *N*-glycans (%)
NS0	Control	60.8	36.2	3.0
	ManNAc (20 m*M*)	58.8	37.2	4.0
	GlcN (10 m*M*) + Urd (2 m*M*)	63.8	32.9	3.3
CHO	Control	60.6	28.0	11.4
	ManNAc (20 m*M*)	58.8	33.4	7.8
	GlcN (10 m*M*) + Urd (2 m*M*)	34.9	43.0	22.1

Cell cultures were adjusted to the indicated final concentration of precursor after 24-h cell growth and cell-free supernatant was harvested 48 h later. Data derived from analyses of 2-aminobenzamide-labeled *N*-glycans by normal phase HPLC (as shown in Fig. 2). All values represent the mean of duplicate cell culture experiments.

α1,3-Gal per mole *N*-glycan in Table III. α-Linked galactosylation was also calculated as a percent of the respective degree of antennarity (assuming termination of all antennae with β1,4-linked Gal acceptor sites), expressed as percent α-galactosylation in Table III. Thus, for control GS-NS0 cells, approximately 33% of *N*-glycan antennae were α-galactosylated (Table III).

Sialylation of released *N*-glycans was analyzed quantitatively both with respect to total degree of sialylation and type of sialic acids present. Degree of sialylation was determined by cation-exchange HPLC, as described previously (Goldman et al., 1998). Typical data are shown in Figure 4 and a comparison of the proportion of differently sialylated oligosaccharides associated with TIMP-1 proteins from control GS-NS0 and GS-CHO cells is shown in Table II. There was a distinctly lower proportion of neutral, nonsialylated oligosaccharides in the NS0-derived population than are present in the CHO-derived pool. This is compensated by an elevated proportion of monosialylated *N*-glycans in the NS0 population. These data were used to derive molar sialic acid content, expressed as moles SA per mole *N*-glycan in Table III. As for sialylation, α-galactosylation was also calculated as a percent of the respective degree of antennarity (assuming termination of all antennae in β1,4-linked Gal acceptor sites), expressed as percent sialylation in Table III. For NS0-derived *N*-glycans, antennae may terminate in either α1,3-Gal *or* sialic acid. It has previously been demonstrated that α1,3-Gal residues cannot be sialylated by mammalian sialyltransferases (Gilbert et al., 1997). Thus, our calculations assume that these glycosyltransferase reactions actually *compete* for free β1,4-Gal acceptor sites, as has been demonstrated previously (Smilovitch et al., 1998; Smith et al., 1990). Even with these considerations, the percent sialylation of TIMP-1 derived from control NS0 cells (53.3%) was slightly greater (by ~5%) than that observed for CHO-derived TIMP-1. Oligosaccharide substitution with particular sialic acid variants was analyzed quantitatively by reverse-phase HPLC of DMB-labeled sialic acids released by mild acid hydrolysis. These data (Fig. 5 and Table IV) demonstrate conclusively that, while CHO-cell-derived *N*-glycans were substituted predominantly with *N*-acetylneuraminic acid (Neu5Ac; >83 %), NS0-derived *N*-glycans were associated with similar proportions of *N*-glycolyl and *N*-acetyl variants. In both cases, there was a minor proportion (<2%) of doubly acetylated neuraminic acid (Neu5,7Ac$_2$).

Sialyltransferase Activity in GS-NS0 and GS-CHO Cells

Associated with the analytical data just examined, total sialyltransferase activity extracted from GS-NS0 and GS-CHO cells was determined in vitro by measurement of the rate of addition of CMP-fluoresceinyl-NeuAc substrate to an asialoglycoprotein acceptor. In each case, sialyltransfer-

Table II. Effect of nucleotide-sugar precursor addition to cultures of GS-NS0 and GS-CHO cells on the sialylation of *N*-glycans associated with recombinant TIMP-1.

Treatment group		Neutral *N*-glycans (%)	Monosialylated *N*-glycans (%)	Bisialylated *N*-glycans (%)	Trisialylated *N*-glycans (%)	Tetrasialylated *N*-glycans (%)
NS0	Control	11.9	50.6	34.6	2.8	0.1
	ManNAc (20 m*M*)	10.7	49.5	36.5	3.0	0.3
	GlcN (10 m*M*) + Urd (2 m*M*)	16.6	50.9	30.1	2.4	0
CHO	Control	29.9	27.5	35.8	6.3	0.5
	ManNAc (20 m*M*)	27.3	32.7	32.9	5.8	1.3
	GlcN (10 m*M*) + Urd (2 m*M*)	30.2	34.7	27.6	5.8	1.7

Cell cultures were adjusted to the indicated final concentration of precursor after 24-h cell growth and cell-free supernatant was harvested 48 h later. Data derive from analyses of 2-aminobenzamide labeled *N*-glycans by cation-exchange HPLC (Fig. 4). All values represent the mean of duplicate cell culture experiments.

10970290, 2001, 3, Downloaded from https://analyticalsciencejournals.onlinelibrary.wiley.com/doi/10.1002/bit.1051 by University Of Manitoba, Wiley Online Library on [25/10/2024]. See the Terms and Conditions (https://onlinelibrary.wiley.com/terms-and-conditions) on Wiley Online Library for rules of use; OA articles are governed by the applicable Creative Commons License

RIGHTSLINK

Table III. Summary of the effect of nucleotide-sugar precursor addition to cultures of GS-NS0 and GS-CHO cells on antennarity, sialylation, and α-galactosylation of *N*-glycans associated with recombinant TIMP-1.

	Treatment group	Mean antennae per *N*-glycan	moles α-Gal/ mol *N*-glycan	α-Galacto sylation (%)	Moles SA/ mol *N*-glycan	Sialylation (%)
NS0	Control	2.42	0.80	33.1	1.29	53.3
	ManNAc (20 m*M*)	2.45	0.89	36.3	1.33	54.3
	GlcN (10 m*M*) + Urd (2 m*M*)	2.40	0.74	30.8	1.19	49.6
CHO	Control	2.51	—	—	1.20	47.8
	ManNAc (20 m*M*)	2.49	—	—	1.21	48.6
	GlcN (10 m*M*) + Urd (2 m*M*)	2.87	—	—	1.14	39.7

In each case the mean number of antennae per *N*-glycan is derived from data presented in Table I. Values relating to *N*-glycan sialylation were calculated using the data shown in Table II (moles SA/mol *N*-glycan) and the associated degree of *N*-glycan antennarity (percent sialylation of β-Gal acceptor sites). Similarly, values relating to *N*-glycan α-galactosylation were calculated using data derived from the normal phase HPLC analyses exemplified in Figure 2 (moles α1,3-linked Gal/mol *N*-glycan) and the associated degree of *N*-glycan antennarity (percent α-galactosylation of β-Gal acceptor sites).

ase activity was measured after 36- and 72-h cell growth in triplicate. Under the assay conditions employed, a significantly higher level of activity was extracted from NS0 cells than CHO cells (after 36 h: GS-NS0, 10.1 ± 0.05 pU cell^{-1}; GS-CHO, 1.43 ± 0.15 pU cell^{-1}; after 72 h: GS-NS0, 13.3 ± 0.10 pU cell^{-1}; GS-CHO, 6.1 ± 0.02 pU cell^{-1}). We note that 1 pU cell^{-1} is equivalent to a rate of sialylation of 1440 fmol of NeuAc transferred per day.

Effect of Nucleotide-Sugar Precursors on *N*-Glycosylation of Recombinant TIMP-1 in GS-NS0 and GS-CHO Cells

We hypothesized that elevation of intracellular CMP-NeuAc content induced by feeding the precursor *N*-acetylmannosamine (ManNAc; as previously demonstrated by Gu and Wang [1998]) would result in an increase in sialylation of *N*-glycans in both cell types. Furthermore, in NS0 cells, elevated CMP-NeuAc would result in: (i) an increase in the proportion of NeuAc rather than NeuGc on *N*-glycans (i.e., a lower proportion of the cellular CMP-NeuAc would be converted to NeuGc by limited intracellular CMP-NeuAc hydroxylase activity); and (ii) decreased α-galactosylation, as sialyltransferases and α-galactosyltransferases are thought to compete for β-Gal acceptor sites. We compared cell-specific controls on *N*-glycan processing by the feeding cells with glucosamine plus uridine (GlcN + Urd). Urd was included to counter cellular depletion of UTP. Treatment with GlcN has been reported to increase intracellular UDP-*N*-acetylhexosamine (UDP-HexNAc) content in BHK-21 cells, resulting in increased *N*-glycan

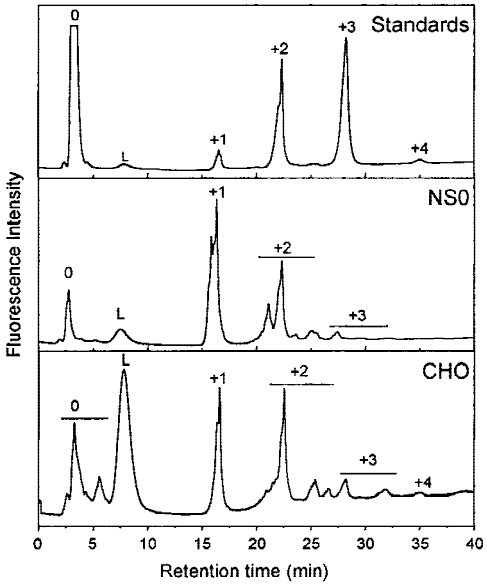

Figure 4. Analysis of the sialylation of fluorophore-labeled *N*-glycans released from recombinant TIMP-1 produced in GS-NS0 and GS-CHO cells by cation-exchange HPLC. Sialylated *N*-linked oligosaccharides were released by digestion with peptide-*N*-glycosidase F, derivatized with 2-aminobenzamide at the reducing terminus and separated by cation-exchange HPLC. Typical separations of neutral (0), monosialylated (+1), disialylated (+2), trisialylated (+3), and tetrasialylated (+4) *N*-glycans from NS0 and CHO-cell-derived recombinant TIMP-1 are shown. L indicates the elution of free 2-aminobenzamide label.

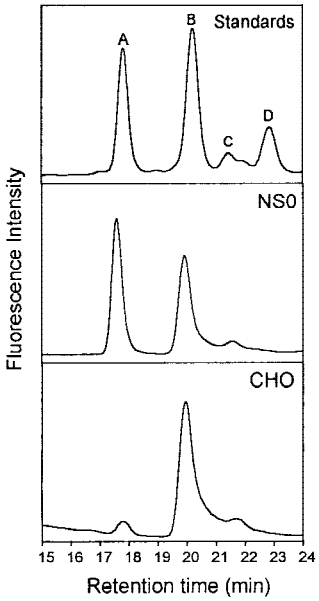

Figure 5. Analysis of sialic acid variants associated with GS-NS0- and GS-CHO-cell-derived recombinant TIMP-1 by reverse-phase HPLC. Sialic acids were released from TIMP-1 *N*-glycans by mild acid hydrolysis, labeled with the fluorophore 1,2-diamino-4,5-methylenedioxybenzene (DMB), and separated by rpHPLC. DMB-labeled standards as follows: (A) Neu5Gc; (B) Neu5Ac; (C) Neu5,7Ac$_2$; and (D) Neu5GcAc9.

10970290, 2001, 3, Downloaded from https://analyticalsciencejournals.onlinelibrary.wiley.com/doi/10.1002/bit.1051 by University Of Manitoba, Wiley Online Library on [25/10/2024]. See the Terms and Conditions (https://onlinelibrary.wiley.com/terms-and-conditions) on Wiley Online Library for rules of use; OA articles are governed by the applicable Creative Commons License

RIGHTSLINK

Table IV. Effect of addition of nucleotide-sugar precursor to cultures of GS-NS0 and GS-CHO cells on the substitution of recombinant TIMP-1 *N*-glycans with sialic acid variants.

Treatment group		Neu5Ac (%)	Neu5,7Ac$_2$ (%)	Neu5Gc (%)
NS0	Control	46.0	1.7	52.3
	ManNAc (20 m*M*)	69.4	0.8	29.8
	GlcN (10 m*M*) + Urd (2 m*M*)	42.2	3.5	54.3
CHO	Control	83.5	1.3	15.2
	ManNAc (20 m*M*)	90.8	2.1	7.1
	GlcN (10 m*M*) + Urd (2 m*M*)	72.8	1.7	25.5

Cell cultures were adjusted to the indicated final concentration of precursor after 24-h cell growth and cell-free supernatant was harvested 48 h later. Data derived from analyses of DMB-labeled sialic acids by reverse-phase HPLC (Fig. 5). All values represent the mean of duplicate analyses.

antennarity and decreased terminal sialylation (Gawlitzek et al., 1998; Grammatikos et al., 1998). Therefore, we expected to observe elevated α1,3-galactosylation of *N*-glycans produced by NS0 cells.

As shown in Table V, addition of 20 m*M* ManNAc to both GS-NS0 and GS-CHO cell cultures after 24-h cell growth markedly stimulated intracellular CMP-sialic acid content measured 48 h later. In both cell types, intracellular CMP-sialic acid levels increased significantly; by 30-fold in GS-NS0 cells and 12-fold in GS-CHO cells. ManNAc treatment did not result in significant alterations in intracellular UDP-HexNAc content (the HPLC technique employed cannot distinguish between UDP-*N*-acetylglucosamine and UDP-*N*-acetylgalactosamine), although UDP-Hex (UDP-glucose + UDP-galactose) levels were decreased by 60% in GS-NS0 cells. However, for *N*-glycans released from recombinant TIMP-1 produced by either GS-NS0 or GS-CHO cells, elevated intracellular ManNAc was not associated with a significant difference in the distribution of differently sialylated oligosaccharides (Table II). For both cell types, only a slight elevation in degree of sialylation was observed (Table III), although this was still not significantly different from the degree to which control TIMP-1 was sialylated. Furthermore, treatment with 20 m*M* ManNAc had no significant effect on *N*-glycan antennarity for both cell types (Tables I and III), and the degree to which *N*-glycans were α-galactosylated in NS0 cells was not significantly elevated (a 3% increase; Table III). In contrast, as shown in Table IV, addition of ManNAc to NS0 cells had a significant effect ($P < 0.05$) on the substitution of *N*-glycans with both NeuAc and NeuGc. In fact, the proportion of Neu5Gc recovered from TIMP-1 oligosaccharides dropped from a mean value of 52% to 30%, with a corresponding increase in the proportion of Neu5Ac. A similar trend was observed for CHO-cell-derived TIMP-1 *N*-glycans, albeit to a much reduced and insignificant extent.

Addition of 10 m*M* GlcN + 2 m*M* Urd to both GS-NS0 and GS-CHO cells led to significant increases in intracellular UDP-HexNAc levels. In GS-NS0 cells, cellular UDP-HexNAc was elevated 18-fold, and in the GS-CHO cells UDP-HexNAc was elevated 60-fold. In addition, in both cell types, mean CMP-NeuAc content was increased approximately 5-fold (GS-NS0) or 2-fold (GS-CHO). In both cell types, UDP-Hex content was also markedly elevated by some 3-fold (GS-NS0) or 8-fold (GS-CHO). Associated with these alterations in nucleotide-sugar metabolism were cell-type-specific changes in *N*-glycan processing. Although the mean antennarity of oligosaccharides associated with TIMP-1 from NS0 cells was unaltered (Tables I and III), *N*-glycans released from CHO-cell-derived TIMP-1 were significantly ($P < 0.05$) more branched. As shown in Table I, both tri- and tetraantennary *N*-glycans were more abundant after treatment of the GS-CHO cells with GlcN + Urd. Notably, the proportion of tetraantennary oligosaccharides increased almost threefold. Consequently, there was a 14% increase in the mean number of antennae per *N*-glycan (Table III). No other alterations to core TIMP-1 *N*-glycan structures were induced by GlcN + Urd treatment of CHO

Table V. Effect of nucleotide-sugar precursor addition to cultures of GS-NS0 and GS-CHO cells on intracellular content of nucleotide-sugars.

Treatment group		CMP-SA (fmol/cell)	UDP-HexNAc (fmol/cell)	UDP-Hex (fmol/cell)
NS0	Control	0.08	0.60	0.24
	ManNAc (20 m*M*)	2.21	0.50	0.10
	GlcN (10 m*M*) + Urd (2 m*M*)	0.39	10.80	0.70
CHO	Control	0.06	0.24	0.10
	ManNAc (20 m*M*)	0.74	0.20	0.07
	GlcN (10 m*M*) + Urd (2 m*M*)	0.12	14.00	0.84

Cell cultures were adjusted to the indicated final concentration of precursor after 24-h cell growth and cells were harvested and analyzed 48 h later. Data derived from analyses of nucelotide-sugars by anion-exchange HPLC (as described in Materials and Methods section, but not shown). All values are the mean of duplicate cell culture experiments.

10970290, 2001, 3, Downloaded from https://analyticalsciencejournals.onlinelibrary.wiley.com/doi/10.1002/bit.1051 by University Of Manitoba, Wiley Online Library on [25/10/2024]. See the Terms and Conditions (https://onlinelibrary.wiley.com/terms-and-conditions) on Wiley Online Library for rules of use; OA articles are governed by the applicable Creative Commons License

RIGHTSLINK

cells, and α-galactosylation of NS0-derived TIMP-1 was not altered significantly (−3%; α-galactosylation of β-gal acceptor sites [Table III]) in NS0 cells.

The sialylation of TIMP-1 *N*-glycans (available β-Gal acceptor sites, taking changes in oligosaccharide antennarity into account) by NS0 cells was moderately (but not significantly) reduced by GlcN + Urd treatment (−4%). However, for CHO cells, the reduction in sialylation was more pronounced. Significantly elevated antennarity of *N*-glycans induced by the GlcN + Urd supplement (+13 %), combined with an insignificant decrease (−5%) in molar sialylation (moles SA per mole *N*-glycan^{-1} [Table III]) resulted in an 8% reduction in the percent sialylation of available β-Gal acceptor sites. Finally, the relative proportion of sialic acid variants (Neu5Ac, Neu5Gc, or Neu5,7Ac$_2$) on NS0-derived TIMP-1 *N*-glycans was not significantly altered with GlcN + Urd treatment. However, CHO-derived *N*-glycans exhibited an increased proportion (+10%) of the Neu5Gc variant following GlcN + Urd supplement.

DISCUSSION

Comparative Analysis of *N*-Glycosylation in GS-NS0 and GS-CHO Cells

Our data demonstrate that the only major differences between NS0-derived and CHO-derived recombinant TIMP-1 were the presence of terminal α1,3-linked galactose and *N*-glycolylneuraminic acid residues on the NS0-derived oligosaccharides. These differences are presumably due to the presence (α1,3-galactosyltransferase) or greater abundance (CMP-NeuAc hydroxylase) of the respective enzymes in the NS0 host cell. In contrast to this study, α1,3-linked galactose residues have been reported to occur to a minor extent on NS0-derived recombinant IgG molecules (Sheeley et al., 1997). However, *N*-glycan processing is sterically hindered at the partially buried Asn$_{297}$ site in the Fc region of IgG (Wormald et al., 1997), so the total extent to which this may occur in NS0 cells was not apparent in this study. As up to 1% of all circulating human IgG is directed against the Galα1,3Gal motif (Galili et al., 1993), antibodies produced by murine cells that carry this epitope have a short half-life in vivo (Borrebaeck et al., 1993). Therefore, current NS0 cell lines are restricted to the production of IgG at present. Our attempts to reduce the occurrence of Galα1,3Gal by a metabolic strategy is described below.

With respect to NeuGc, the extent to which *N*-glycans are sialylated with either NeuAc or NeuGc residues is now known to be highly species specific. For example, Raju et al. (2000) recently analyzed sialylated IgG *N*-glycans from a variety of species and found that the relative proportions of NeuAc and NeuGc varied considerably (mouse-derived IgG contained only NeuGc). In this study, while NeuGc was prevalent on NS0-derived *N*-glycans (>60%), we also observed a reasonably high proportion of NeuGc on CHO *N*-glycans (15%). This exceeds the low proportion (1% to 5%) of NeuGc previously reported for recombinant proteins produced by CHO cells (Hokke et al., 1995), and may be specific to this cell line. As CMP-NeuAc hydroxylase is not present in humans (Irie and Suzuki, 1998; Muchmore et al., 1989), NeuGc is considered to be potentially immunogenic (Noguchi et al., 1995). Therefore, *N*-glycan substitution with NeuGc is undesirable, even for recombinant IgG proteins where sialylation is reduced by steric hindrance. Our studies indicate that NS0 cells will sialylate *N*-glycans with NeuGc, although substitution with NeuGc can be reduced considerably by metabolic means, as described below. Furthermore, there is the possibility that elimination of both α1,3-galactosyltransferase and CMP-NeuAc hydroxylase activities in NS0 cells may be achieved by direct genetic manipulation (Gregoire et al., 1998; Shinkel et al., 1997).

Effect of *N*-Acetylmannosamine on Cell Growth and *N*-Glycosylation

In agreement with recent previous reports concerned with CHO cells (Gu and Wang, 1998; Zanghi et al., 1998), we found that a ManNAc supplement (20 m*M* in this study) substantially increased the CMP-sialic acid content of both NS0 and CHO cells. Associated with this was a decline in the UDP-Hex content of both cell types, more evident in NS0 cells than in CHO cells. In addition, in both cell types, there was a slight decline in UDP-HexNAc level, indicating a general trend toward reduction in cellular UDP-sugar content with ManNAc treatment. In unsupplemented cells, endogenous ManNAc may be derived from UDP-GlcNAc via UDP-GlcNAc-2-epimerase or from GlcNAc via GlcNAc-2-epimerase. As the former reaction is subject to negative feedback control by CMP-NeuAc, a ManNAc supplement effectively bypasses this control step, which normally regulates CMP-NeuAc production (Fig. 6). However, synthesis of CMP-sialic acids also requires a source of cytidine triphosphate, which may be derived either from CDP directly or alternatively from UTP plus glutamine by an ATP-dependent reaction catalyzed by CTP synthetase yielding CTP plus glutamate (Koerner, 1970). CTP synthetase is known to be upregulated in tumor cells (Hatse et al., 1999). As we did not supply ManNAc with cytidine, we speculate that this nucleotide may have become limiting and that the alternative source of CTP from UTP and glutamine via CTP synthetase may have competed for cellular UTP, partially compromising UTP-sugar synthesis. Moreover, Nyberg et al. (1999) postulated that glutamine limitation itself may compromise UDP-GlcNAc synthesis as Gln is the amino donor for glucosamine-6-phosphate synthesis from fructose-6-phosphate (Fig. 6). In both cell types, these ManNAc-induced alterations in UDP-sugar metabolism were not of sufficient magnitude to induce changes in *N*-glycosylation of recombinant TIMP-1; core antennarity and galactosylation were effectively unchanged.

We expected to see an increase in the degree of sialylation of TIMP-1 *N*-glycans derived from NS0 and CHO cells treated with ManNAc via increased CMP-NeuAc

RIGHTSLINK

10970290, 2001, 3, Downloaded from https://analyticalsciencejournals.onlinelibrary.wiley.com/doi/10.1002/bit.1051 by University Of Manitoba, Wiley Online Library on [25/10/2024]. See the Terms and Conditions (https://onlinelibrary.wiley.com/terms-and-conditions) on Wiley Online Library for rules of use; OA articles are governed by the applicable Creative Commons License

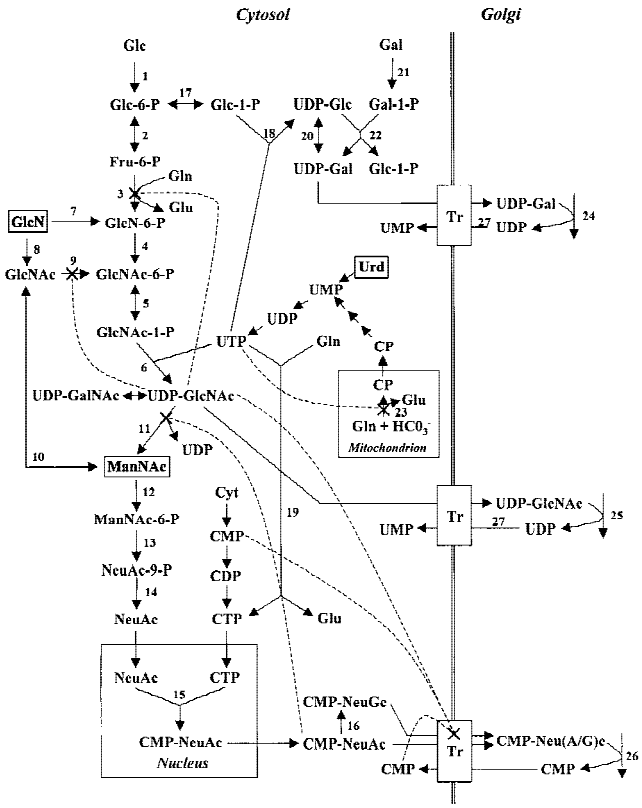

Figure 6. Primary metabolic interconversions and controls implicated in nucleotide-sugar biosynthesis and transport in mammalian cells. The metabolic precursors supplied in the present study are highlighted. Broken lines terminating in a cross link a synthesis or transport process with the potential regulatory metabolite (Carey et al., 1980; Pels Rijcken et al., 1995; Ryll et al., 1994, Valley et al., 1999). CP, carbamoyl phosphate; Tr, nucleotide-sugar transporter. Numbered enzymes as follows: 1, hexokinase; 2, phosphoglucose isomerase; 3, GlcN-6-P synthase; 4, GlcN-6-P *N*-acetyltransferase; 5, GlcNAc-6-P mutase; 6, UDP-GlcNAc pyrophosphorylase; 7, hexokinase; 8, GlcN *N*-acetyltransferase; 9, GlcNAc kinase; 10, GlcNAc-2-epimerase; 11, UDP-GlcNAc-2-epimerase; 12, ManNAc kinase; 13, NeuAc-9-P synthase; 14, NeuAc phosphatase; 15, CMP-NeuAc synthetase; 16, CMP-NeuAc-4-hydroxylase; 17, phosphoglucomutase; 18, UDP-Glc pyrophosphorylase; 19, CTP synthetase; 20, UDP-Gal-4-epimerase; 21, galactokinase; 22, Gal-1-P uridyltransferase; 23, carbamoylphosphate synthetase II; 24, galactosyltransferases (α1,3 or β1,4); 25, GlcNAc transferases (I to V); 26, sialyltransferases (α2,3 and α2,6); 27, nucleoside diphosphatase.

availability. However, this was not the case. In fact, the extent of *N*-glycan sialylation was virtually unchanged after ManNAc treatment, despite augmented cellular CMP-NeuAc levels. These data concur with those previously observed for ManNAc-treated CHO cells (Gu and Wang, 1998; Zanghi et al., 1998), which also demonstrated a limited effect of ManNAc treatment and significantly elevated intracellular CMP-NeuAc levels on recombinant protein sialylation. These data imply that CMP-NeuAc availability in the Golgi lumen may be a factor limiting the effect of ManNAc in both cell types. CMP-sialic acid may occur in three distinct subcellular compartments; it is synthesized in the nucleus and transported from the cytosol to the lumen of the *trans*-Golgi network via a specific transporter (Berninsone et al., 1997; Eckhardt and Gerardy-Schahn, 1997; Munster et al., 1998). Although we have not quantified CMP-sialic acid in these discrete subcellular locations, it has been suggested that CMP-sialic acid transport capacity into the Golgi lumen is intrinsically limited (Carey et al., 1980) and inhibited by UDP-HexNAc or CMP (Cacan et al., 1984; Pels Rijcken et al., 1995).

Despite the fact that the NS0 (and most mammalian) cells contained α1,3-galactosyltransferase activity, which is thought to compete for β1,4-Gal acceptor sites with endogenous sialyltransferases (Smilovitch et al., 1998; Smith et al., 1990), sialylation of the NS0-derived TIMP-1 slightly exceeded that of the CHO-derived TIMP-1. However, sialyltransferase (ST) activity present in NS0 cells (α2,3- *and* α2,6-ST) was double that present in the CHO cells (known to contain α2,3-ST only). Therefore, if we consider that α1,3-Gal residues cannot be sialylated (Gilbert et al., 1997), then the observed level of sialylation in NS0 cells may have been promoted by higher endogenous sialyltransferase activity. However, in control NS0 cells, α-galactosylation and sialylation together accounted for only 86% of β1,4-Gal acceptor sites, not 100%. As discussed, CMP-NeuAc availability in the Golgi may also intrinsically limit sialylation and, while UDP-Gal levels in the Golgi lumen may not limit β-galactosyltransferase activity, there is some evidence that α-galactosyltransferase has a lower affinity for UDP-Gal than does β-galactosyltransferase (Hara et al., 1989; Kawakita et al., 1998). Finally, we do not discount the possibility that a soluble form of α1,3-galactosyltransferase occurs in murine NS0 cells (Cho and Cummings, 1997). Thus, α-galactosyltransferase and sialyltransferase reactions may actually "compete" in the Golgi to only a limited extent. Genetic augmentation of sialyltransferase activity in mammalian cells has not consistently increased the total sialic acid content of glycoproteins. Although Weikert et al. (1999) demonstrated that overexpression of α2,3-sialyltransferase in CHO cells resulted in increased glycoprotein sialylation (>90% of branches), expression of α2,6-sialyltransferase in BHK-21 cells had no such effect, although α2,6-linked sialic acids were present (Grabenhorst et al., 1995).

The other factor that could affect the observed degree of sialylation of recombinant TIMP-1 produced by *both* NS0 and CHO cells is specific productivity; that is, elevated specific productivity effectively introduces additional competing β1,4-Gal acceptor sites into the Golgi lumen. Even taking account of differences between cell types, this may be significant. For example, the GS-CHO cell line had a specific productivity in excess of 20 μg 10^6 cells^{-1} day^{-1} with approximately 50% of outer arm β1,4-Gal residues sialylated. Therefore, there are three basic variables that may affect the extent of *N*-glycan sialylation in mammalian cells expressing a recombinant protein with a sterically unhindered glycosylation site: (i) availability of sialyltransferase activity; (ii) abundance of β1,4-Gal acceptor sites (related to cell specific productivity); and (iii) availability of nucleotide-sugar substrate in the Golgi lumen. The latter factor may be a significant determinant. Whereas incom-

10970290, 2001, 3, Downloaded from https://analyticalsciencejournals.onlinelibrary.wiley.com/doi/10.1002/bit.1051 by University Of Manitoba, Wiley Online Library on [25/10/2024]. See the Terms and Conditions (https://onlinelibrary.wiley.com/terms-and-conditions) on Wiley Online Library for rules of use; OA articles are governed by the applicable Creative Commons License

RIGHTSLINK

plete sialylation may be considered to be "built in" to cellular *N*-glycan processing for a variety of biological purposes (Varki, 1993), it follows that rational genetic improvement of sialylation (at least in CHO cells) could involve augmentation of CMP-sialic acid transport into the Golgi via elevated expression of recently cloned CMP-NeuAc transporter genes (Eckhardt and Gerardy-Schahn, 1997; Ishida et al., 1998). This is a strategy that we are currently testing in this laboratory.

Finally, although increased sialylation was not associated with elevated CMP-NeuAc, we observed clear differences in the proportion of sialic acid variants substituted on NS0- and CHO-derived *N*-glycans. The same trend occurred with both cell types treated with ManNAc, albeit to a greater (and significant) extent with NS0 cells — that is, an increase in the proportion of NeuAc over NeuGc. We interpret this simply as a saturation of limited soluble cytosolic CMP-NeuAc hydroxylase (monooxygenase) activity in the cell (Muchmore et al., 1989). This is therefore a modification that is under direct control of available enzyme activity *and* substrate. A similar manipulation of cell metabolism by incorporation of a synthetic precursor, *N*-glycolylmannosamine pentacetate, in the growth environment of neural cells has recently been shown to result in an increase in the proportion of Neu5Gc associated with a myelin-associated glycoprotein, decreasing its biological activity (Collins et al., 2000).

Effect of Glucosamine on Cell Growth and *N*-Glycosylation

In common with many previous reports (Gawlitzek et al., 1998; Grammatikos et al., 1998; Zanghi et al., 1998), we observed that addition of glucosamine to both GS-NS0 and GS-CHO cell cultures resulted in an inhibition of cell growth and metabolism with a concomitant increase in cellular UDP-HexNAc content. Indeed, there is now very strong evidence to suggest that glucosamine exerts this influence primarily through its direct incorporation into cellular UDP-GlcNAc. It is thought that stimulation of UDP-GlcNAc synthesis by glucosamine, as observed for both cell types employed in the present study (we cannot distinguish between UDP-GlcNAc and UDP-GalNAc), may in turn trap UTP in an enlarged UDP-GlcNAc pool, resulting in a deficiency of this nucleotide. Alternatively, it has recently been speculated (Valley et al., 1999) that altered intracellular UDP-GlcNAc levels may affect the degree to which nuclear and cytoplasmic proteins are modified by O-GlcNAc residues. This form of O-glycosylation may be involved in the regulation of a variety of cellular processes (e.g., transport of proteins between nucleus and cytoplasm) (Haltiwanger et al., 1992; Hart et al., 1996). The latter hypothesis is more attractive, as it has previously been shown that inhibition of the growth of colon carcinoma cells in culture by glucosamine was associated with elevated UDP-GlcNAc *without* a decrease in cellular UTP or CTP pools (Krug et al., 1984). Moreover, in the present study, simultaneous addition of uridine with glucosamine (specifically to counter potential UTP depletion) did not eliminate the reduction in cell growth. Furthermore, a similar limiting deficiency in the cellular CTP pool may have been expected on supplementation of cell cultures with ManNAc, which markedly stimulated CMP-sialic acid synthesis in NS0 and CHO cells, possibly "trapping" cellular cytidine in the process. In this case, decreased cell growth did not occur.

Recent studies using baby hamster kidney (BHK)-21 cells have clearly established a link between elevated cellular UDP-HexNAc level and alterations in *N*-glycan processing, specifically increased *N*-glycan antennarity and decreased sialylation (Gawlitzek et al., 1998; Grammatikos et al., 1998; Valley et al., 1999). The former is thought to be the result of increased transport of UDP-GlcNAc substrate into the Golgi lumen with a consequent stimulation of the activity of GlcNAc transferases IV and V. It has been suggested that the latter may be mediated by an inhibition of CMP-sialic acid transport into the Golgi lumen by UDP-GlcNAc (Pels Rijcken et al., 1995).

Furthermore, Ryll (1994) have shown that UDP-GlcNAc forms a partial link between the inhibitory effect of ammonia on cell growth and *N*-glycosylation. Recently, using $^{15}NH_{4^+}$, Valley et al. (1999) demonstrated conclusively that extracellular ammonium is incorporated into cellular UDP-GlcNAc and recombinant protein *N*-glycans. However, ammonium (derived from glutamine metabolism and/or degradation), being a weak base, may also raise the pH of acidic cellular compartments, such as the Golgi affecting nucleotide-sugar transporters (Hirschberg, 1997) and/or the activity of lumenal glycosyltransferases (Thorens and Vassalli, 1986). In recent studies, Wagner and colleagues (Gawlitzek et al., 1998; Grammatikos et al., 1998) suggested that, in BHK-21 cells, ammonium ions act by these independent mechanisms to regulate antennarity (via elevated UDP-GlcNAc) and sialylation (via elevated Golgi pH). Even relatively small increases in extracellular ammonia have been associated with alterations in *N*-glycan processing. Andersen and Goochee (1995) reported that sialylation of the O-glycans associated with granulocyte colony stimulating factor was compromised by NH_{4^+} concentrations up to 2 m*M*. It is of interest to note that the CMP-NeuAc transporter recently isolated by complementation cloning of mutant (Lec2) CHO cells bears a structural similarity to cloned ammonium transporters (Eckhardt et al., 1996; Marini et al., 1994). In contrast, both NS0 and CHO cell lines employed in the present study expressed the recombinant TIMP-1 gene under glutamine synthetase (GS) selection/amplification. Aside from relatively high-level gene expression (>20 μg 10^6 cells^{-1} day^{-1} in both cases), these cell lines do not accumulate ammonia as they are necessarily maintained in a glutamine-free environment and any ammonia generated metabolically is recycled in the synthesis of glutamine from glutamate. Consequently, extracellular ammonia never exceeded 0.15 m*M* in either NS0 or CHO cultures. Under these conditions, we consider our experi-

10970290, 2001, 3, Downloaded from https://analyticalsciencejournals.onlinelibrary.wiley.com/doi/10.1002/bit.1051 by University Of Manitoba, Wiley Online Library on [25/10/2024]. See the Terms and Conditions (https://onlinelibrary.wiley.com/terms-and-conditions) on Wiley Online Library for rules of use; OA articles are governed by the applicable Creative Commons License

RIGHTSLINK

ments to have occurred in essentially "ammonia-free" conditions. However, the GS-NS0 and GS-CHO cell cultures may be considered to be intrinsically glutamine-limited (endogenous GS in CHO cells is inhibited by methionine sulfoximine), and, as stated earlier, glutamine limitation itself may impose constraints on UDP-GlcNAc synthesis (Nyberg et al., 1999; Fig. 6). For example, we previously observed higher cell-specific levels of UDP-HexNAc in experiments using glutamine-containing CHO cell cultures producing recombinant interferon-γ under DHFR selection/amplification (Hooker et al., 1999).

Although the data we obtained for GS-CHO cells supports the hypothesis that increased cellular UDP-GlcNAc induced by a GlcN + Urd supplement promotes *N*-glycan antennarity by a stimulation of UDP-GlcNAc transport into the Golgi, the same cannot be inferred for GS-NS0 cells. In this cell type, *N*-glycan branching was not affected. There may be numerous effectors influencing this observation, including cell-type variations in: (i) the abundance or affinity of a particular Golgi transporter or glycosyltransferase for its nucleotide-sugar substrate; (ii) affinity of glycosyltransferases for a particular acceptor substrate; (iii) nucleotide-sugar synthesis pathways and effectors; (iv) competition between adjacent Golgi glycosyltransferases; (v) glycosyltransferase cofactor levels (e.g., Mn^{2+}); and (vi) availability of *N*-glycan acceptors (H. Schachter, personal communication).

On treatment of both cell types with GlcN + Urd, we observed an elevation of UDP-Hex levels, presumably as we supplied the Urd supplement to compensate for Urd trapped in increased UDP-HexNAc. We note that, for another GS-NS0 cell line employed in this laboratory (producing a recombinant humanized antibody), the same trend is observed. Furthermore, in the absence of Urd, there is a slight decline in cellular UDP-Hex content with a GlcN supplement alone (unpublished observations). Pels Rijcken et al. (1995) observed a 3.8-fold increase in UDP-Hex levels and a 4.6-fold increase in UDP-HexNAc after treatment of rat hepatocytes with 0.5 m*M* Urd alone for 40 h. Thus, we speculate that the GlcN supplement "pulls" UTP away from UDP-Hex synthesis into a UDP-GlcNAc "sink." Inclusion of a Urd supplement will offset this phenomenon to an extent that varies with cell type, prevailing metabolic balance, and inherent controls. However, as we cannot distinguish between UDP-Gal and UDP-Glc, the possibility remains that the Urd supplement primarily promotes UDP-Glc synthesis and not UDP-Gal, as Glc was the hexose source supplied in culture media. This may explain why increased UDP-Hex does not promote an increase in *N*-glycan α-galactosylation, as observed on treatment of NS0 cells with GlcN +Urd. In these cells, we may have expected an elevation of α-galactosylation given the significantly elevated UDP-Hex substrate levels.

The effect of GlcN + Urd on the degree of terminal sialylation was similar in both cell types, a slight (and insignificant) reduction by 5% to 8%. However, associated with this was an increase in cellular CMP-sialic acid content, also seen in both cell types. These apparently contradictory observations may be explained if we accept the hypothesis that elevated UDP-HexNAc inhibits CMP-sialic acid transport into the Golgi (Pels Rijcken et al., 1995), reducing its rapid incorporation into glycoconjugates by sialyltransferases. Elevated intracellular CMP-sialic acid is likely to derive from a stimulation of ManNAc synthesis (a precursor of CMP-NeuAc) by GlcN. This may occur biosynthetically in two ways: (i) UDP-GlcNAc is a substrate for UDP-GlcNAc-2-epimerase, yielding ManNAc; and (ii) conversion of GlcNAc to ManNAc by GlcNAc-2-epimerase (Fig. 6). Given that the UDP-GlcNAc-2-epimerase is subject to negative feedback inhibition by CMP-NeuAc in a concentration-dependent manner (Hinderlich et al., 1997), elevated CMP-NeuAc will downregulate its own de novo synthesis via this route. Similar considerations would also apply to the CMP-sialic acid transporter in the Golgi.

The proportions of sialic acid variants associated with TIMP-1 were not affected by GlcN + Urd treatment of NS0 cells. Conversely, the GS-CHO-cell-derived TIMP-1 exhibited an increased proportion of CMP-NeuGc. Given that the GlcN + Urd-induced increase in cellular CMP–sialic acid was not as marked in GS-CHO cells as in GS-NS0 cells, and that CMP-NeuAc hydroxlase activity is lower in CHO cells, this result is cannot be explained at present.

CONCLUSIONS

We have compared metabolic control of *N*-glycan processing in two mammalian cell types. Our studies confirm that control of *N*-glycan processing is not solely reliant upon the complement, ordered sequence, and abundance of glycosyltransferases in the secretory apparatus, but is also controlled by metabolic and transport processes that affect substrate availability. Our experiments demonstrated that metabolic control of *N*-glycosylation involves processes that are conserved between cell types (e.g., the minimal effect of elevated cellular UDP-HexNAc and CMP-sialic acid on sialylation) and those that are not (e.g., the effect on elevated cellular UDP-HexNAc on *N*-glycan branching). We infer that these cell-specific observations are ultimately a consequence of differences in the kinetics of intermolecular reactions (protein/protein and protein/metabolite) between genetic variants within protein (sub)families.

Strategies to control *N*-glycosylation in mammalian cells for biotechnological purposes may not be based only upon genetic alteration of glycosyltransferase activity (although this can be successful; see Umana et al. [1999] and Weikert et al. [1999]), but also on metabolic considerations. For example, we highlight the possibility that increased transport of CMP-NeuAc into the Golgi lumen by regulated overexpression of the CMP-sialic acid transporter may prove to be a generally effective means of improving sialylation. Furthermore, metabolite feeding strategies may be a viable means of control. For example, *N*-acetymannosamine can significantly reduce *N*-glycan substitution with *N*-glycolylneuraminic acid. This approach could therefore be used to reduce the occurrence of this

10970290, 2001, 3, Downloaded from https://analyticalsciencejournals.onlinelibrary.wiley.com/doi/10.1002/bit.1051 by University Of Manitoba, Wiley Online Library on [25/10/2024]. See the Terms and Conditions (https://onlinelibrary.wiley.com/terms-and-conditions) on Wiley Online Library for rules of use; OA articles are governed by the applicable Creative Commons License

RIGHTSLINK

potential immunogen on recombinant proteins produced by murine cells.

NOMECLATURE

Asn	asparagine
2-AB	2-aminobenzamide
BHK	baby hamster kidney
CH_3CN	acetonitrile
CHO	Chinese hamster ovary
CMP	cytidine monophosphate
CNBr	cyanogen bromide
CTP	cytidine 5′-triphosphate
DHB	2,5-dihydroxybenzoic acid
DMB	1,2-diamino-4,5-methylenedioxybenzene
Fc	constant region of immunoglobulin molecule
FCS	fetal calf serum
Gal	galactose
Glc	glucose
GlcN	glucosamine
GlcNAc	*N*-acetylglucosamine
GS	glutamine synthetase
Hex	hexose
HexNAc	*N*-acetylhexosamine
ManNAc	*N*-acetylmannosamine
MALDI-TOF MS	matrix-assisted laser desorption ionization time-of-flight mass spectrometry
MeOH	methanol
NeuAc	*N*-acetylneuraminic acid
NeuGc	*N*-glycolylneuraminic acid
PBS	phosphate-buffered saline
PNGase F	peptide-*N*-glycosidase F
PVDF	polyvinyldifluoride membrane
rpHPLC	reverse-phase high-pressure liquid chromatography
SA	sialic acid
SDS-PAGE	sodium dodecylsulfate–polyacylamide gel electrophoresis
TIMP-1	tissue inhibitor of metalloproteinases 1
t_d	doubling time
UDP	uridine 5′-diphosphate
Urd	uridine
UTP	uridine 5′-triphosphate
μ	specific growth rate

References

Andersen DC, Goochee CF. 1995. The effect of ammonia on the O-linked glycosylation of granulocyte colony stimulating factor produced by Chinese hamster ovary cells. Biotechnol Bioeng 47:96–105.

Baker K, Ison A, Freedman R, Jones W, James D. 1997. Real-time monitoring of recombinant protein concentration in animal cell cultures using an optical biosensor. Gen Eng Biotechnol 17:69–74.

Berninsone P, Eckhardt M, Gerardy-Schahn R, Hirschberg CB. 1997. Functional expression of the murine Golgi CMP-sialic acid transporter in *Saccharomyces cerevisiae*. J Biol Chem 272:12616–12619.

Bigge JC, Patel TP, Bruce JA, Goulding PN, Charles SM, Parekh RB. 1995. Nonselective and efficient fluorescent labeling of glycans using 2-aminobenzamide and anthranilic acid. Anal Biochem 230:229–238.

Borrebaeck CAK, Malmborg AC, Ohlin M. 1993. Does endogenous glycosylation prevent the use of mouse monoclonal-antibodies as cancer therapeutics? Immunol Today 14:477–479.

Cacan R, Cecchelli R, Hoflack B, Verbert A. 1984. Intralumenal pool and transport of CMP-*N*-acetylneuraminic acid, GDP-fucose and UDP-galactose — study with plasma-membrane-permeabilized mouse thymocytes. Biochem J 224:277–284.

Carey DJ, Sommers LW, Hirschberg CB. 1980. CMP-*N*-acetylneuraminic acid: Isolation from and penetration into mouse liver microsome. Cell 19:597–605.

Cho SK, Cummings RD. 1997. A soluble form of alpha 1,3-galactosyltransferase functions within cells to galactosylate glycoproteins. J Biol Chem 272:13622–13628.

Cockett MI, Bebbington CR, Yarranton GT. 1990. High level expression of tissue inhibitor of metalloproteinases in Chinese hamster ovary cells using glutamine synthetase gene amplification. Bio/Technology 8: 662–667.

Collins BE, Fralich TJ, Saki I, Ichikawa Y, Schnaar RL. 2000. Conversion of cellular sialic acid expression from N-acetyl- to N-glycolylneuraminic acid using a synthetic precursor, *N*-glycolylmannosamine pentaacetate: inhibition of myelin-associated glycoprotein binding to neural cells. Glycobiology 10:11–20.

Eckhardt M, Gerardy-Schahn R. 1997. Molecular cloning of the hamster CMP-sialic acid transporter. Eur J Biochem 248:187–192.

Eckhardt M, Muhlenhoff V, Bethe A, Gerardy-Schahn R. 1996. Expression cloning of the Golgi CMP-sialic acid transporter. Proc Natl Acad Sci USA 93:7572–7576.

Galili U, Anaraki F, Thall A, Hillblack C, Radic M. 1993. One percent of human girculating B-lymphocytes are capable of producing the natural anti-gal antibody. Blood 82:2485–2493.

Gawlitzek M, Valley U, Wagner R. 1998. Ammonium ion and glucosamine dependent increases of oligosaccharide complexity in recombinant glycoproteins secreted from cultivated BHK-21 cells. Biotechnol Bioeng 57:518–528.

Gilbert M, Cunningham AM, Watson DC, Martin A, Richards JC, Wakarchuk WW. 1997. Characterization of a recombinant *Neisseria meningitidis* alpha-2,3-sialyltransferase and its acceptor specificity. Eur J Biochem 249:187–194.

Goldman MH, James DC, Rendall MH, Ison AP, Hoare M, Bull AT. 1998. Monitoring N-glycosylation of recombinant human interferon-γ produced during perfused fluidized-bed and batch culture of CHO cells. Biotechnol Bioeng 60:596–607.

GomisRuth FX, Maskos K, Betz M, Bergner A, Huber R, Suzuki K, Yoshida N, Nagase H, Brew K, Bourenkov GP, Bartunik H, Bode W. 1997. Mechanism of inhibition of the human matrix metalloproteinase stromelysin-1 by TIMP-1. Nature 389:77–81.

Grabenhorst E, Hoffmann A, Nimtz M, Zettlmeissl G, Conradt HS. 1995. Construction of stable BHK-21 cells coexpressing human secretory glycoproteins and human gal(beta-1–4)GlcNAc-r-alpha-2,6-sialyltransferase. alpha-2,6-linked NeuAc is preferentially attached to the gal(beta-1–4)GlcNAc(beta-1–2)man(alpha-1–3)-branch of diantennary oligosaccharides from secreted recombinant beta-trace protein. Eur J Biochem 232:718–725.

Grabenhorst E, Schlenke P, Pohl S, Nimtz M, Conradt HS. 1999. Genetic engineering of recombinant glycoproteins and the glycosylation pathway in mammalian host cells. Glycoconjug J 16:81–97.

Grammatikos SI, Valley U, Nimtz M, Conradt HS, Wagner R. 1998. Intracellular UDP-*N*-acetylhexosamine pool affects *N*-glycan complexity: A mechanism of ammonium action on protein glycosylation. Biotechnol Progr 14:410–419.

Gregoire A, Visvikis A, Marc A, Goergen J-L. 1998. Antisense RNA for the elimination of NeuGc residues from recombinant glycoproteins. In: Merten O-W, Perrin P, Griffiths B, editors. New developments and new applications in animal cell technology: Proceedings of the 15th ESACT meeting. Dordrecht: Kluwer. p 191–193.

Gu XJ, Wang DIC. 1998. Improvement of interferon-gamma sialylation in Chinese hamster ovary cell culture by feeding of *N*-acetylmannosamine. Biotechnol Bioeng 58:642–648.

Guile GR, Rudd PM, Wing DR, Prime SB, Dwek RA. 1996. A rapid high-resolution high-performance liquid-chromatographic method for separating glycan mixtures and analyzing oligosaccharide profiles. Anal Biochem 240:210–226.

Haltiwanger RS, Blomberg MA, Hart GW. 1992. Glycosylation of nuclear and cytoplasmic proteins — purification and characterization of a uridine diphospho-*N*-acetylglucosamine-polypeptide beta-N-acetylglucosaminyltransferase. J Biol Chem 267:9005–9013.

10970290, 2001, 3, Downloaded from https://analyticalsciencejournals.onlinelibrary.wiley.com/doi/10.1002/bit.1051 by University Of Manitoba, Wiley Online Library on [25/10/2024]. See the Terms and Conditions (https://onlinelibrary.wiley.com/terms-and-conditions) on Wiley Online Library for rules of use; OA articles are governed by the applicable Creative Commons License

RIGHTSLINK

Hara T, Endo T, Furukawa K, Kawakita M, Kobata A. 1989. elucidation of the phenotypic change on the surface of Had-1 cell, a mutant-cell line of mouse Fm3a carcinoma-cells selected by resistance to Newcastle-disease virus-infection. J Biochem 106:236–247.

Hart GW, Kreppel LK, Comer FI, Arnold CS, Snow DM, Ye ZY, Cheng XG, Dellamanna D, Caine DS, Earles BJ, Akimoto Y, Cole RN, Hayes BK. 1996. *O*-GlcNAcylation of key nuclear and cytoskeletal proteins — reciprocity with *O*-phosphorylation and putative roles in protein multimerization. Glycobiology 6:711–716.

Hatse S, DeClercq E, Balzarini J. 1999. Role of antimetabolites of purine and pyrimidine nucleotide metabolism in tumor cell differentiation. Biochem Pharmacol 58:539–555.

Hinderlich S, Stasche R, Zeitler R, Reutter W. 1997. A bifunctional enzyme catalyzes the first two steps in *N*-acetylneuraminic acid biosynthesis of rat liver — purification and characterization of UDP-*N*-acetylglucosamine 2-epimerase/N-acetylmannosamine kinase. J Biol Chem 272:24313–24318.

Hirschberg CB. 1997. Transporters of nucleotide sugars, nucleotide sulfate and ATP in the Golgi apparatus membrane: Where next? Glycobiology 7:169–171.

Hokke CH, Bergwerff AA, Vandedem GWK, Kamerling JP, Vliegenthart JFG. 1995. Structural analysis of the sialylated *N*-linked and *O*-linked carbohydrate chains of recombinant-human-erythropoietin expressed in chinese-hamster ovary cells — sialylation patterns and branch location of dimeric *N*-acetylactosamine units. Eur J Biochem 228: 981–1008.

Hooker AD, Green NH, Baines AJ, Bull AT, Jenkins N, Strange PG, James DC. 1999. Constraints on the transport and glycosylation of recombinant IFN-γ in Chinese hamster ovary and insect cells. Biotechnol Bioeng 63:559–572.

Irie A, Suzuki A. 1998. CMP-*N*-acetylneuraminic hydroxylase is exclusively inactive in humans. Biochem Biophys Res Commun 248: 330–333.

Ishida N, Ito M, Yoshioka S, SunWada GH, Kawakita M. 1998. Functional expression of human Golgi CMP–sialic acid transporter in the Golgi complex of a transporter-deficient Chinese hamster ovary cell mutant. J Biochem 124:171–178.

James DC, Baker KN. 1999. Glycosylation of recombinant proteins. In: Flickinger MC, Drew SW, editors. Encyclopedia of bioprocess technology: Fermentation, biocatalysis and bioseparation. New York: John Wiley & Sons. p 1336–1349.

James DC, Freedman RB, Hoare M, Ogonah OW, Rooney BC, Larionov OA, Dobrovolsky VN, Lagutin OV, Jenkins N. 1995. *N*-glycosylation of recombinant human interferon-gamma produced in different animal expression systems. Bio/Technology 13:592–596.

James DC, Jenkins N. 1997. Analysis of *N*-glycans by matrix assisted laser desorption/ionisation mass spectrometry. In: Jackson P, Gallagher JT, editors. A laboratory guide to glycoconjugate analysis. Basel: Birkhauser. p 91–112.

Jefferis R, Lund J. 1997. Glycosylation of antibody molecules: structural and functional significance. Chem Immunol 65:111–128.

Jenkins N, Parekh RB, James DC. 1996. Getting the glycosylation right: Implications for the biotechnology industry. Nature Biotechnol 14: 975–981.

Kawakita M, Ishida N, Miura N, SunWada GH, Yoshioka S. 1998. Nucleotide sugar transporters: Elucidation of their molecular identity and its implication for future studies. J Biochem 123:777–785.

Koerner JF. 1970. Enzymes of nucleic acid metabolism. Ann Rev Biochem 39:291–322.

Krug E, Zweibaum A, Schulzholstege C, Keppler D. 1984. D-Glucosamine-induced changes in nucleotide metabolism and growth of colon carcinoma cells in culture. Biochem J 217:701–708.

Lavecchio JA, Dunne AD, Edge ASB. 1995. Enzymatic removal of alpha-galactosyl epitopes from porcine endothelial cells diminishes the cytotoxic effect of natural antibodies. Transplantation 60:841–847.

Lifely MR, Hale C, Boyce S, Keen MJ, Phillips J. 1995. Glycosylation and biological activity of Campath-1H expressed in different cell-lines and grown under different culture conditions. Glycobiology 5:813–822.

Marini AM, Vissers S, Urrestarazu A, Andre B. 1994. Cloning and expression of the Mep1 gene encoding an ammonium transporter in *Saccharomyces cerevisiae*. EMBO J 13:3456–3463.

Marzowski J, Wang WC, Flesher AR, Raff HV. 1995. Fluorophore-labeled carbohydrate analysis of immunoglobulin fusion proteins — correlation of oligosaccharide content with in vivo clearance profile. Biotechnol Bioeng 46:399–407.

Monica TJ, Williams SB, Goochee CF, Maiorella BL. 1995. Characterization of the glycosylation of a human IgM produced by a human–mouse hybridoma. Glycobiology 5:175–185.

Muchmore EA, Milewski M, Varki A, Diaz S. 1989. Biosynthesis of *N*-glycolyneuraminic acid — the primary site of hydroxylation of *N*-acetylneuraminic acid is the cytosolic sugar nucleotide pool. J Biol Chem 264:20216–20223.

Munster AK, Eckhardt M, Potvin B, Muhlenhoff M, Stanley P, Gerardy-Schahn R. 1998. Mammalian cytidine 5′-monophosphate *N*-acetylneuraminic acid synthetase: A nuclear protein with evolutionarily conserved structural motifs. Proc Natl Acad Sci USA 95: 9140–9145.

Noguchi A, Mukuria CJ, Suzuki E, Naiki M. 1995. Immunogenicity of *N*-glycolylneuraminic acid-containing carbohydrate chains of recombinant human erythropoietin expressed in Chinese hamster ovary cells. J Biochem 117:59–62.

Nyberg GB, Balcarcel RR, Follstad BD, Stephanopoulos G, Wang DIC. 1999. Metabolic effects on recombinant interferon-γ glycosylation in continuous culture of chinese hamster ovary cells. Biotechnol Bioeng 62:336–347.

Papac DI, Briggs JB, Chin ET, Jones AJS. 1998. A high-throughput microscale method to release, *N*-linked oligosaccharides from glycoproteins for matrix-assisted laser desorption/ionization time-of-flight mass spectrometric analysis. Glycobiology 8:445–454.

Pels Rijcken WRP, Overdijk B, Vandeneijnden DH, Ferwerda W. 1995. The effect of increasing nucleotide sugar concentrations on the incorporation of sugars into glycoconjugates in rat hepatocytes. Biochem J 305:865–870.

Raju TS, Briggs JB, Borge SM, Jones AJS. 2000. Species specific variation in glycosylation of IgG: Evidence for the species-specific sialylation and branch–specific galactosylation and importance for engineering recombinant glycoprotein therapeutics. Glycobiology 10:477–489.

Rudd PM, Guile GR, Kuster B, Harvey DJ, Opdenakker G, Dwek RA. 1997. Oligosaccharide sequencing technology. Nature 388:205–207.

Ryll T, Valley U, Wagner R. 1994. Biochemistry of growth inhibition by ammonium ions in mammalian cells. Biotechnol Bioeng 44:184–193.

Sheeley DM, Merrill BM, Taylor LCE. 1997. Characterization of monoclonal antibody glycosylation: Comparison of expression systems and identification of terminal alpha-linked galactose. Anal Biochem 247: 102–110.

Shinkel TA, Chen CG, Salvaris E, Henion TR, Barlow H, Galili U, Pearse MJ, d'Apice AJF. 1997. Changes in cell surface glycosylation in alpha 1,3-galactosyltransferase knockout and alpha 1,2-fucosyltransferase transgenic mice. Transplantation 64:197–204.

Smilovich D, Malagolini N, Fagioli C, deLalla C, Sitia R, Serafini Cessi F. 1998. Differential expression of Gal alpha 1,3Gal epitope in polymeric and monomeric IgM secreted by mouse myeloma cells deficient in alpha 2,6-sialyltransferase. Glycobiology 8:841–848.

Smith DF, Larsen RD, Mattox S, Lowe JB, Cummings RD. 1990. Transfer and expression of a murine UDP-gal-beta-D-gal-alpha-1,3-galactosyltransferase gene in transfected Chinese hamster ovary cells — competition reactions between the alpha-1,3-galactosyltransferase and the endogenous alpha-2,3-sialyltransferase. J Biol Chem 265: 6225–6234.

Sutton CW, Oneill JA, Cottrell JS. 1994. Site-specific characterization of glycoprotein carbohydrates by exoglycosidase digestion and laser-desorption mass-spectrometry. Anal Biochem 218:34–46.

Thorens B, Vassalli P. 1986. Chloroquine and ammonium chloride prevent terminal glycosylation of immunoglobulins in plasma cells without affecting secretion. Nature 321:618–620.

Umana P, Jean Mairet J, Moudry R, Amstutz H, Bailey JE. 1999. Engi-

10970290, 2001, 3, Downloaded from https://analyticalsciencejournals.onlinelibrary.wiley.com/doi/10.1002/bit.1051 by University Of Manitoba, Wiley Online Library on [25/10/2024]. See the Terms and Conditions (https://onlinelibrary.wiley.com/terms-and-conditions) on Wiley Online Library for rules of use; OA articles are governed by the applicable Creative Commons License

RIGHTSLINK

neered glycoforms of an antineuroblastoma IgG1 with optimized antibody-dependent cellular cytotoxic activity. Nature Biotechnol 17: 176–180.

Valley U, Nimtz M, Conradt HS, Wagner R. 1999. Incorporation of ammonium into intracellular UDP-activated *N*-acetylhexosamines and into carbohydrate structures in glycoproteins. Biotechnol Bioeng 64: 401–417.

Varki A. 1993. Biological roles of oligosaccharides — all of the theories are correct. Glycobiology 3:97–130.

Weikert S, Papac D, Briggs J, Cowfer D, Tom S, Gawlitzek M, Lofgren J, Mehta S, Chisholm V, Modi N, Eppler S, Carroll K, Chamow S, Peers D, Berman P, Krummen L. 1999. Engineering Chinese hamster ovary cells to maximise sialic acid content of recombinant glycoproteins. Nature Biotechnol 17:1116–1121.

Wormald MR, Rudd PM, Harvey DJ, Chang SC, Scragg IG, Dwek RA. 1997. Variations in oligosaccharide–protein interactions in immunoglobulin G determine the site-specific glycosylation profiles and modulate the dynamic motion of the Fc oligosaccharides. Biochemistry 36:1370–1380.

Zanghi JA, Mendoza TP, Schmelzer AE, Knop RH, Miller WM. 1998. Role of nucleotide sugar pools in the inhibition of NCAM polysialylation by ammonia. Biotechnol Progr 14:834–844.

RIGHTSLINK

10970290, 2001, 3, Downloaded from https://analyticalsciencejournals.onlinelibrary.wiley.com/doi/10.1002/bit.1051 by University Of Manitoba, Wiley Online Library on [25/10/2024]. See the Terms and Conditions (https://onlinelibrary.wiley.com/terms-and-conditions) on Wiley Online Library for rules of use; OA articles are governed by the applicable Creative Commons License